

A possible prediction method to determine the top concealed karst cave based on displacement monitoring during tunnel construction

S. C. Li¹ · J. Wu¹ · Z. H. Xu¹ · L. Zhou¹ · B. Zhang¹

Received: 19 November 2016 / Accepted: 21 April 2017 / Published online: 23 May 2017
© Springer-Verlag Berlin Heidelberg 2017

Abstract The existence of concealed karst caves can cause major displacement and even large deformation of surrounding rock during karst tunnel excavation. As such, these concealed caves pose a large threat to the stability of surrounding rock and represent major hidden threats to safe tunnel construction. Here we report on our investigation of a possible method to predict the top of a concealed karst cave based on displacement monitoring during tunnel construction. Displacement laws of monitoring sections were analyzed and compared to a case study without karst caves after the tunnel was excavated once. Numerical calculation was carried out to verify the proposed method. The impacts of a number of factors were studied by taking into account the effects of displacement fields, such as tunnel depth, the surrounding rock grade, the size of the karst cave, the distance between the tunnel and the karst cave and the depth–span ratio of the karst cave, on the stability of surrounding rock in tunnels. Compared with the case study without karst caves, the surrounding rock deformation affected by the top karst cave during tunnel excavation is discussed, and

simulation results were found to be consistent with those predicted by the proposed method. These research results can provide a new concepts for comprehensive forecasting techniques of the concealed karst cave.

Keywords Karst tunnel · Concealed karst cave · Displacement monitoring · Prediction method · Monitoring surface

Introduction

The presence of concealed karst caves poses a great threat to tunnel construction and subsequent operational safety due to the potential for water and mud inrush, collapse, and other serious geological disasters which may occur during the excavation of karst tunnels (Cooper 1998; White 2002; Day 2004; Liu et al. 2007; Fu and Feng 2012; Gutierrez et al. 2014; Fu et al. 2015; Pan and Dias 2015; Li et al. 2016). Therefore, research on the stability of the rock surrounding a tunnel (hereafter referred to as surrounding rock in tunnels) as affected by concealed karst caves has very important scientific and practical significance (White 2002; Day 2004; Gutierrez et al. 2014; Shrestha and Panthi 2015; Lin et al. 2017).

In the early days of tunneling, engineering analogy methods and empirical methods were adopted to analyze these issues (Zou 1994; Chen and He 2004). However, such methods resulted in large man-made differences, which represent major potential security risks to tunnel construction (Runqiu and Huabo 2010; Taromi et al. 2016). More recent research has led many experts and scholars to believe that the existence of concealed karst caves can make surrounding rock in tunnels produce distortion (Liu et al. 2003). If the rock stratum thickness between the karst cave and the tunnel reaches a critical safety thickness, the surrounding rock will

✉ S. C. Li
lishuca@sdu.edu.cn

J. Wu
wujing9516@163.com

Z. H. Xu
zhenhao_xu@sdu.edu.cn

L. Zhou
18769788330@163.com

B. Zhang
zhangbo1977@sdu.edu.cn

¹ Geotechnical and Structural Engineering Research Center, Shandong University, Ji'nan, Shandong 250061, China

lose its stability and fail, with subsequent water inrush, mud inrush, collapse, among other consequences. Chen et al. (2004) proposed a coupled creep damage model based on the elasto-plastic constitutive model and applied this model to analyze the stability of a large underground powerhouse cavern. The field measurements and numerical simulation performed by these authors confirmed the validity of the model. Yang et al. (2004) modeled tunneling-induced ground surface movements using the stochastic medium theory. The formulated ground movement equations were then used to perform back analyses of 18 ground surface settlement profiles available in the literature. Liu et al. (2004) built geometric models of polyhedral key blocks based on block theory which comprehensively considered the action of gravity and dynamic loadings and then analyzed the stability of a key block of a large underground excavation. Song (2006) simplified the top karst cave to a beam-slab model and then deduced the numerical solution of the minimum safe thickness of the tunnel roof and floor by adopting elastic theory. Lai (2012) analyzed the safe distance between the concealed karst cave and the tunnel based on the strength reduction method, energy catastrophe theory and dichotomy. A comparison of these three methods led the author to conclude that the numerical solution of catastrophe theory was the most reasonable.

With recent advances in technology, development of the finite element method and improvement in computer processing capability, present-day engineers and researchers use large-scale finite element analysis softwares, such as ANSYS, FLAC2D/3D, RFPA, MIDAS, etc., to research the stability of the surrounding rock in tunnels. In a simulation study, Zhao et al. (2004) studied how the size of karst caves can affect the stability of the surrounding rock in tunnels by using ANSYS; the simulated results were verified by carrying out similarity model tests. The results showed that the deformation of surrounding rock in tunnels increased with karst cave size and that the excavation of tunnels with karst caves amplified the deformation of the surrounding rock without karst caves. Sterpi and Cividini (2004) looked at the behavior of tunnels up to failure of shallow underground openings on the basis of a number of small-scale model tests carried out in the laboratory and finite element simulation. The comparison between experimental and numerical results led the authors to draw a number of conclusions on the influence of strain localization, the overall behavior of shallow tunnels and the stability of their headings. Parise and Lollino (2011) explored the progression of instability of karst caves by numerical analyses, also analyzing and modeling factors leading to underground failures. For more information on various methods, the author is referred to other sources (including Wang and Fan 2000; Knez and Slabe (2002); Hu and Huang 2007; Song et al. 2008; Mo and Zhou 2008; Mo 2009; Tan et al. 2009; Zhao et al. 2014).

Conventional studies often focus on the stability of surrounding rock in tunnels as affected by karst caves. However, how to predict concealed karst caves on the basis of a stability study is often ignored. Relevant research is also seldom related to the specific work of predicting karst caves based on displacement monitoring. If the location of karst caves can be timely and effectively predicted during tunnel construction, specific control principles and relevant treatment measures can be made—and disastrous consequences potentially avoided. Thus, research on methods to predict concealed karst caves based on displacement monitoring during tunnel construction has very important theoretical significance and engineering value.

The mechanics mechanism of surrounding rock in tunnels is affected differently depending on the location of the karst cave. The effects of bottom karst caves on tunnel stability are relatively smaller than those of caves at other locations for the following reasons. Vertical displacements of the tunnel arch foot and the tunnel floor are large, and bracing requirements of the tunnel floor are high. Stress concentration may be found in the vicinity of the tunnel arch foot and the tunnel floor (Liu et al. 2003). The effects of top karst caves on tunnel stability are mainly those of vault subsidence. The maximum principal stress of the tunnel roof varies with the location of karst caves. The self-supporting capacity of vault surrounding rock should be strengthened in time during excavation. The strength requirements for surrounding rock in tunnels and lining structure are higher for top karst caves than for bottom karst caves, and the disasters which have occurred involving the former are also larger (Wang and Fan 2000; Sterpi and Cividini 2004; Day 2004; Hu and Huang 2007). We have therefore taken the top concealed karst cave as an example and researched a possible prediction method of the top concealed karst cave based on displacement monitoring during tunnel construction. The reasons for “possible” are as follows. If a concealed karst cave exists above the proposed tunnel, the monitored results in tunneling are consistent with those predicted by the proposed method. On the contrary, if the monitored results in tunneling are consistent with those predicted by the proposed method, owing to other excavation influence factors, there can be no guarantee that a concealed karst cave actually exists above the proposed tunnel. However, the proposed method provide supplementary data to facilitate the prediction of concealed karst caves during advance geological forecasts of the tunnel.

In the study reported here we analyzed the deformation laws of the surrounding rock in tunnels and compared the results with a case study without karst caves after the tunnel is excavated once, which is discussed in Section 2.1. Engineering application methods for predicting the top concealed karst cave are proposed and described in Section 2.2. In order to verify the proposed method, we researched the excavation stepwise based on numerical simulation. Displacement laws of the tunnel arch ring monitoring points at different monitoring distance s (behind the tunnel

face) are analyzed, as detailed in Section 3.1. Five class case studies are carried out in Section 3.2, and some are compared with the case study without karst caves. The surrounding rock deformation as affected by the top karst cave during tunnel excavation is analyzed and discussed. A number of main conclusions are drawn in Section 4.

The possible prediction method of the top concealed karst cave

Monitoring measurements of surrounding rock during karst tunnel excavation is a strategy often adopted to investigate the deformation of surrounding rock in tunnels. According to the general rules of conventional monitoring measurement, the existence of concealed karst caves has effects on the deformation of surrounding rock in tunnels and, in the case of the top concealed karst cave, can cause tunnel vault subsidence and floor heave. Such monitoring is performed one tunnel section at a time during tunnel excavation. Consequently, the aim of this study was to examine a prediction method of the top concealed karst cave by monitoring multiple tunnel sections at one time during tunnel construction.

Deformation law of the surrounding rock

In order to investigate the prediction method of the top concealed karst cave based on displacement monitoring, the deformation law of surrounding rock in tunnels was studied after the tunnel was excavated once.

Numerical model

A three-dimensional tunnel model was built by using the finite element software ANSYS and then carrying out the calculation of tunnel excavation by importing the data into the finite difference software FLAC3D. Many factors have to be considered, and a simple and quick modeling process can be provided in ANSYS; as well, the grid cell can be meshed reasonably according to different spatial patterns of karst cave. Thus, a series of models can be built based on the change of each factor. The calculation can be carried out successively in FLAC3D by setting reasonable parameters.

The geometrical model of this study is determined based on the calculation principle of tunnel structure, a relevant case study, in situ geological conditions and construction situations. The whole-model dimension is as follows. In the horizontal direction (x -axis) and vertical direction (y -axis), 50 m is taken respectively along the positive and negative directions. In the thickness direction (z -axis), 60 m is taken along the negative direction. The starting center of the planned tunnel is located at the origin of coordinates, i.e., $x = 0$, $y = 0$, $z = 0$.

The span of the tunnel (x -direction) is 11.6 m, and its height (y -direction) is 8.83 m. The distance between the tunnel vault and upper boundary of the whole model is 44.2 m. The concealed karst cave is simplified in the shape of a cuboid, which lies right above the planned tunnel. Its center is located at the middle section of the model in the z -direction, i.e., $Z = -30$ m. A mapped face meshing is adopted. The size, shape and position of the karst cave are preset during the modeling. The finite difference model is established, as shown in Fig. 1. There are approximately 100,000 to 200,000 grid cells. Visualization is that the areas of the tunnel section and karst cave are dense, and with the grid gradually becoming sparse towards the surrounding rock. The outermost grid adopts a uniform appearance that meets the requirements of model calculation.

The numerical analysis of the tunnel excavation was carried out in FLAC3D. Boundary conditions were set as follows. Vertical displacement constraints were imposed on the lower boundary, and horizontal displacement constraints were imposed on the left and right boundaries. Axial displacement constraints were imposed on the forward and backward boundaries. The Druck–Prager yield criterion was adopted during the calculations, and the elastic–plastic model was used for problem solving.

Mechanical parameters of the surrounding rock in tunnels were obtained from geological survey data and compared to several engineering sites (Xu et al. 2001; Cai et al. 2002; Song 2006; Mo 2009; Fu and Feng 2012; Lai 2012) (Table 1).

In the numerical simulation, tunnel depth is set as follows. First, the simulation of initial gravity stress of the tunnel is conducted based on the whole geometrical models. Then, the remaining tunnel depth is determined by applying equivalent uniform distributed load onto the top of the models. During excavation, the karst cave is first excavated in the pre-set

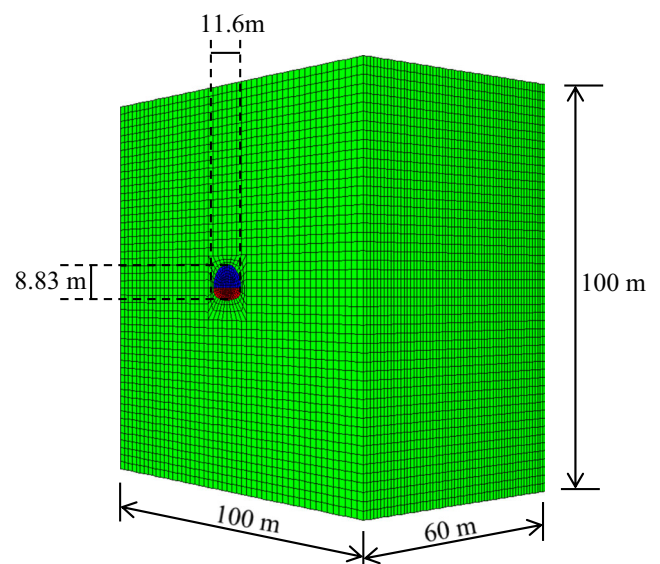


Fig. 1 The finite difference model and mesh generation

Table 1 Mechanical parameters of the tunnel surrounding rock

Surrounding rock grade	Gravity (KN/m ³)	Elastic modulus (GPa)	Poisson's ratio	Internal friction angle (°)	Cohesion (MPa)	Tensile strength (MPa)
I	27	20	0.22	60	2.0	2.0
II	27	15	0.23	50	1.8	1.5
III	26	6	0.28	40	1.2	1.5
IV	25	3	0.32	30	0.8	0.6
V	24	2	0.35	25	0.6	0.5

position, and when this is completed, the tunnel excavation can be carried out. In order to investigate predicting mechanism of the top concealed karst cave, one excavation is first adopted in the process of tunnel excavation.

The full face excavation method is used in the tunnel, with the length of the planned tunnel being 60 m. A monitoring section is set at distances of 3 m in the tunnel, with a total of 20 monitoring sections. In addition, four monitoring points are arranged on each monitoring section, i.e., tunnel vault monitoring point #1 (0, 5.8), tunnel haunch monitoring points #2 (−5.8, 0) and #4 (5.8, 0) and tunnel bottom monitoring point #3 (0, 3.03) (Fig. 2a).

Deformation analysis of the surrounding rock

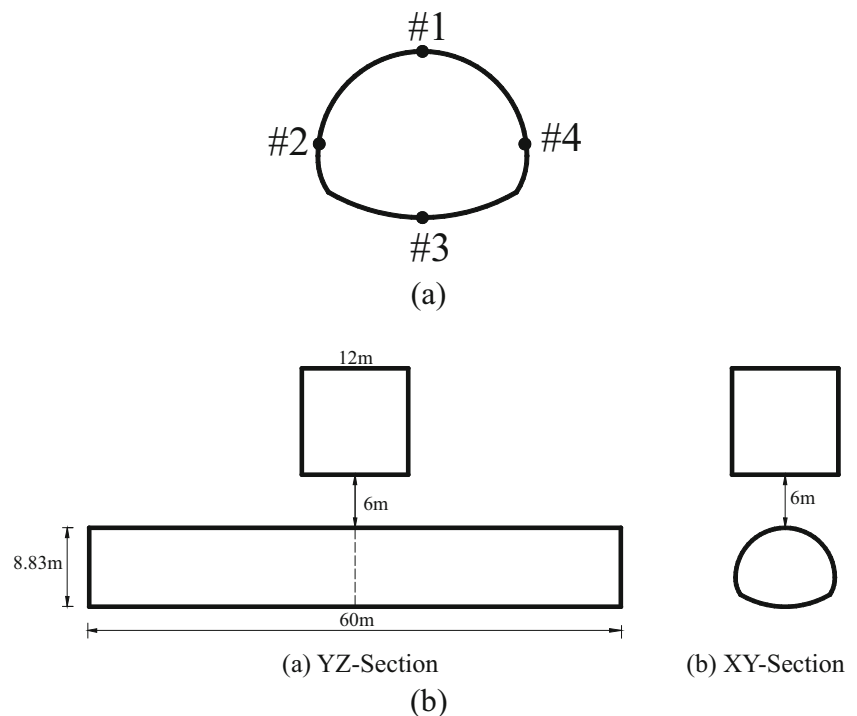
A karst cave was built on the top of the planned tunnel, and its center located at the middle section of the model in the z -direction. The top karst cave ranged in the z -direction from −26 m to −34 m. The model parameters were set at a tunnel depth of 300 m, surrounding rock grade of III, side length of

the karst cave of 12 m, distance between the tunnel and the karst cave of 6 m, and depth–span ratio of the karst cave of 1:1. The relative positions of the top karst cave and the tunnel are shown in Fig. 2b.

The displacement characteristic of each monitoring surface (approx. −60 m) after one excavation was researched. Compared with a case study without karst cave, the displacement rule of each monitoring point was analyzed. Figure 3a shows the Y-displacement of tunnel vault monitoring point #1 under each monitoring surface, Fig. 3b shows the X-displacement of tunnel haunch monitoring point #2 under each monitoring surface and Figure 3c shows the Y-displacement of the tunnel bottom monitoring point #3 under each monitoring surface. It should be noted that “with” represents the case study with the karst cave, and “without” represents the case study without the karst cave.

Similar to the case study without the karst cave, the Y-displacement of tunnel vault monitoring point #1 changed little after one excavation, approximately showing a tendency towards the horizontal line (Fig. 3a). Were a karst cave to be

Fig. 2 Scheme of the arrangement of the tunnel monitoring points and relative positions of the karst cave and the tunnel. **a** Arrangement of the tunnel monitoring points [#1 tunnel vault monitoring point (0, 5.8), #2, #4 tunnel haunch monitoring points (−5.8, 0 and 5.8, 0, respectively), #3 tunnel bottom monitoring point (0, 3.03)], **b** relative positions of the karst cave and the tunnel



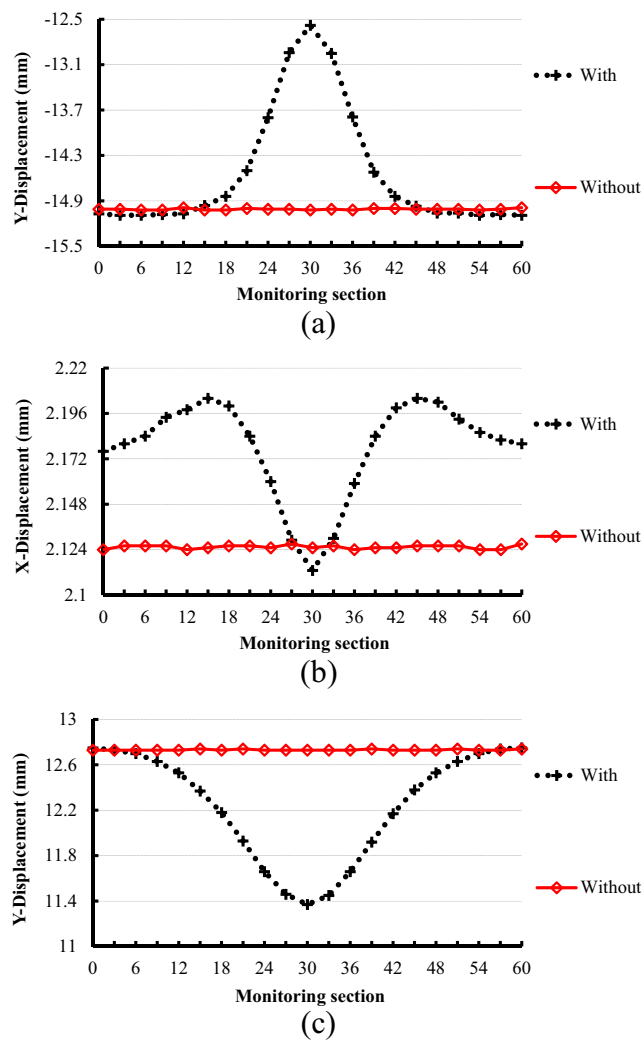


Fig. 3 The displacement of tunnel monitoring points at tunnel vault monitoring point #1 (a), tunnel haunch monitoring point #2 (b) and tunnel bottom monitoring point #3 (c)

present on top of the planned tunnel, the Y-displacement of monitoring point #1 would be symmetrical left and right based on the symmetry axis of $Z = 30$ m. Specifically, the Y-displacement would first decrease then increase. The minimum value is when $Z = 30$ m, and the maximum value is when $Z = 0$ m or $Z = 60$ m. The direction of the whole Y-displacement is downward.

Similar to the case study without the karst cave, the X-displacement the tunnel haunch monitoring point #2 changed gently (Fig. 3b). It is symmetrical left and right based on the symmetry axis of $Z = 30$ m, and it has a minimum value when $Z = 30$ m. Specifically, when Z ranges from 0 to 30 m, the X-displacement of monitoring point #2 first increases and then decreases, then the X-displacement increases gradually, and then the X-displacement decreases gradually. The direction of the whole X-displacement is rightward.

Similar to the case study without the karst cave, the Y-displacement of tunnel bottom monitoring point #3 changes

little after one excavation, showing approximately a tendency towards the horizontal line (Fig. 3c). the Y-displacement of the monitoring point #3 is symmetrical left and right based on the symmetry axis of $Z = 30$ m. To be specific, the Y-displacement first decreases then increases. The value is the minimum when $Z = 30$ m, while it is the maximum when $Z = 0$ m or $Z = 60$ m. The direction of the whole Y-displacement is upward.

Engineering application methods

Based on the above analysis, the prediction method of the top concealed karst cave was used in actual tunnel engineering as described in the following text.

In the course of excavation, let us suppose that the full face excavation method is adopted in the tunnel and that 3 m is excavated every day. After the completion of the excavation of 3 m, the tunnel vault and tunnel bottom monitoring points are arranged on the corresponding tunnel face, as the #1 and #3 in Fig. 2a shows. The excavation is carried out in sequence. A monitoring section is set by every 3 m, and the corresponding monitoring points #1 and #3 are arranged. Meanwhile, vertical displacements of monitoring points #1 and #3 on section of 3 m behind the tunnel face are monitored. Specifically, after the completion of the excavation of 3 m, i.e., after the first day, tunnel vault monitoring point #1 and tunnel bottom monitoring point #3 are arranged on the tunnel face of 3 m. After the completion of excavation of 6 m, i.e., after the second day, tunnel vault monitoring point #1 and tunnel bottom monitoring point #3 are arranged on the tunnel face of 6 m, while at the same time vertical displacements of monitoring points #1 and #3 on the section of 3 m are monitored. After the completion of the excavation of 9 m, i.e., after the third day, tunnel vault monitoring point #1 and tunnel bottom monitoring point #3 are arranged on the tunnel face of 9 m, while at the same time vertical displacements of monitoring points #1 and #3 on the section of 6 m are monitored. The excavation is conducted in sequence, and the displacements of the monitoring points #1 and #3 on the corresponding section are monitored. In this way, the change in vertical displacement of monitoring points #1 and #3 can be obtained during tunnel excavation. These displacement values are drawn in curves for prediction and analysis purposes.

With continuing excavation, the corresponding vertical displacement curves of the tunnel vault monitoring point #1 and tunnel bottom monitoring point #3 are drawn. The appearance of apparent turning points in the two displacement curves with the displacement starting to become smaller can suggest the possible presence of a concealed karst cave in the front of the tunnel face. Based on the decrease of the two vertical displacements, if the variation range of tunnel vault monitoring point #1 is significantly more than that of tunnel bottom monitoring point #3, there is a possibility of a top concealed karst caves in the front of the tunnel face.

If the two displacement curves change gently and show an increasing tendency, it indicates the concealed karst cave is basically not existed in the front of the tunnel face.

Numerical validations

Stepwise excavation

The numerical model described above is used in this section, but a stepwise excavation is adopted in the process of tunnel excavation.

During the stepwise excavation, 3 m is considered to be an excavation step. Taking into account the boundary effect of the model, we selected monitoring sections in the range of approximately 9 to 51 m. The corresponding displacements of the arch ring monitoring points were researched and analyzed. The following four conditions were mainly studied. After the completion of each excavation step (3 m), the displacement of each monitoring point on the 3-, 6-, 9- and 12-m sections behind the tunnel face is monitored. Specially, when the tunnel face is excavated to 21 m, the displacement of each monitoring point on the sections of 18, 15, 12 and 9 m is monitored. When the tunnel face is excavated to 24 m, the displacement of each monitoring point on the sections of 21, 18, 15 and 12 m is monitored. The excavation computation was conducted in sequence and the displacement of each monitoring point monitored, following which the displacement change of each monitoring point can be obtained in the tunnel excavation.

In the course of excavation, the displacements of arch ring monitoring points on monitoring sections of 3, 6, 9 and 12 m behind the tunnel face are drawn in curves. The displacement change of the tunnel arch ring monitoring points at different monitoring distances is obtained. Figure 4a, b, c shows the Y-displacement of tunnel vault monitoring point #1 under different monitoring distances (Fig. 4a), the X-displacement of tunnel haunch monitoring points #2 under different monitoring distances (Fig. 4b) and the Y-displacement of tunnel bottom monitoring point #3 under different monitoring distances (Fig. 4c).

In Fig. 4, the displacement value on the monitoring section of 9 m is expressed as follows:

For the curve of 3 m, it is the displacement value monitored on the section of 9 m when the tunnel face is excavated to 12 m.

For the curve of 6 m, it is the displacement value monitored on the section of 9 m when the tunnel face is excavated to 15 m.

For the curve of 9 m, it is the displacement value monitored on the section of 9 m when the tunnel face is excavated to 18 m.

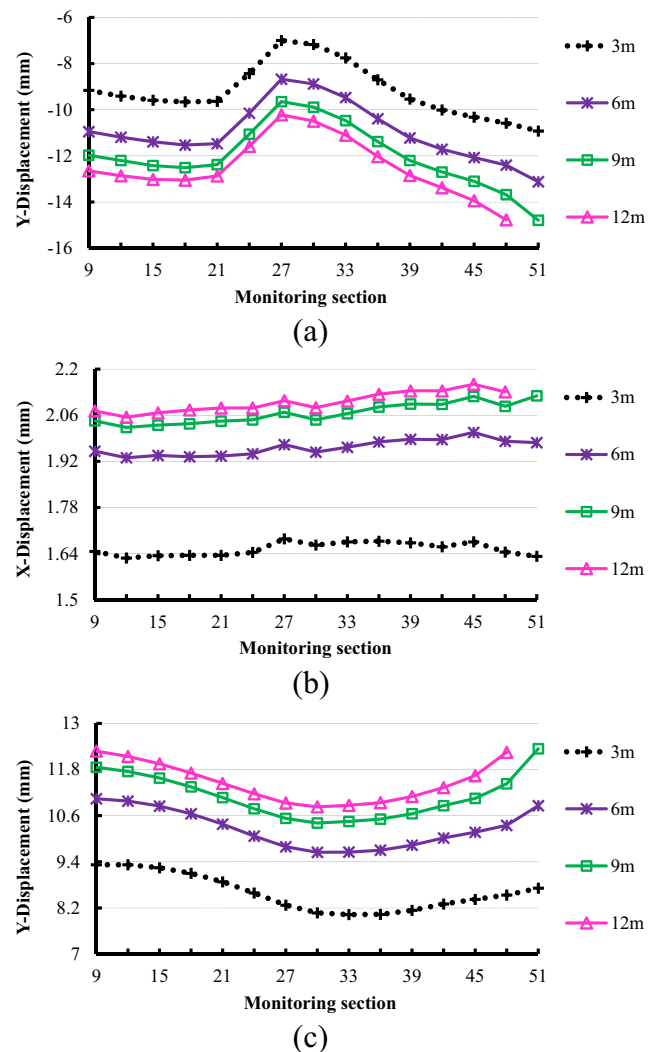


Fig. 4 The displacement of tunnel monitoring points under different monitoring distances. **a** Tunnel vault monitoring point #1, **b** tunnel haunch monitoring point #2, **c** tunnel bottom monitoring point #3

For the curve of 12 m, it is the displacement value monitored on the section of 9 m when the tunnel face is excavated to 21 m.

The remaining curves are constructed in the same manner.

It can be concluded from Fig. 4a that when the range of the monitoring section is from 9 to 21 m, the Y-displacement of tunnel vault monitoring point #1 changes gently. When the range of the monitoring section is from 21 to 27 m, the Y-displacement of monitoring point #1 rapidly decreases, and the displacement variation is larger. The displacement is reduced to a minimum on the monitoring section of 27 m. When the range of monitoring section is from 27 to 51 m, the Y-displacement of monitoring point #1 increases gradually, reaching its maximum value on the monitoring section of 51 m. Overall, the Y-displacement of tunnel vault monitoring

point #1 first decreases and then increases, and its direction is downward. In addition, under the four monitoring distances, as the monitoring distance increases, the Y-displacement of monitoring point #1 also increases gradually, but the increasing range decreases gradually.

It can be concluded from Fig. 4(b) that the X-displacement of tunnel haunch monitoring point #2 changes gently. From a general view, this shows an increasing tendency, and its direction is rightward. In addition, under the four monitoring distances, as the monitoring distance increases, the X-displacement of monitoring point #2 also increases gradually, but the increasing range decreases gradually.

It can be concluded from Fig. 4(c) that when the range of monitoring section is from 9 to 30 m, the Y-displacement of tunnel bottom monitoring point #3 gradually decreases, reaching a minimum value on the monitoring section of 30 m. When the range of monitoring section is from 30 to 51 m, the Y-displacement of monitoring point #3 gradually increases. On the whole, the Y-displacement of tunnel bottom monitoring point #3 first decreases and then increases, and its direction is upward. Furthermore, under the four monitoring distances, as the monitoring distance increases, the Y-displacement of monitoring point #3 also increases gradually, but the increasing range decreases gradually.

Case studies and discussion

Among those factors which affect the stability of surrounding rock in tunnels, we selected tunnel depth, surrounding rock grade, size of the karst cave, the distance between the tunnel and the karst cave, the depth–span ratio of karst cave as research targets. Five case studies involving each influencing factor were simulated and investigated. Simulated working conditions of the top concealed karst cave are listed in Table 2. Their impacts on the stability of surrounding rock in tunnels were studied by taking the displacement field into account. Compared with the case study without karst cave, the surrounding rock deformation affected by the top karst cave during the tunnel excavation was also discussed.

The stepwise excavation was adopted during the tunnel excavation, and 3 m was considered to be an excavation step.

Table 2 Simulated working conditions of the top concealed karst cave

Tunnel depth (m)	Surrounding rock grade	Size of the karst cave (m)	Distance between the tunnel and karst cave (m)	Depth–span ratio of the karst cave
100	I	4	2	6:24
200	II	8	4	8:18
300	III	12	6	1:1
400	IV	16	8	18:8
500	V	20	10	24:6

Monitoring sections in the range of approximately 9 to 51 m were selected to account for the boundary effect of the model. The corresponding displacements of arch ring monitoring points were researched and analyzed. A monitoring distance step of 3 m was adopted—i.e., after completion of each excavation step (3 m), the displacement of each monitoring point on the section of 3 m behind the tunnel face was monitored.

The first class of case studies—different tunnel depths

A karst cave is built on the top of the planned tunnel, and its center is located at the middle section of the model in the Z-direction. The range of the top karst cave in the Z-direction is from -24 to -36 m. In order to investigate the stability of surrounding rock in tunnels affected by the top concealed karst cave under different tunnel depths, we set the tunnel depth to 100, 200, 300, 400 and 500 m, respectively. Median values for the other four influencing factors are chosen and remain unchanged during the modeling, i.e., surrounding rock grade (Grade III), the side length of the karst cave (12 m), the distance between the tunnel and the karst cave (6 m), depth–span ratio of the karst cave (1:1).

The Y-displacement of tunnel vault monitoring point #1 In the course of tunnel excavation, the vertical displacement of tunnel vault monitoring point #1 on each monitoring section is monitored and drawn in curves. Then, the Y-displacement diagram of the tunnel vault monitoring point #1 under different tunnel depths is obtained, as shown in Fig. 5.

- 1) As the tunnel depth increases, the Y-displacement of monitoring point #1 increases gradually, and the extent of variation also increases gradually.
- 2) When the tunnel depth is 100 or 200 m, the Y-displacement of tunnel vault monitoring point #1 changes gently. The displacement shows a minor fluctuation nearby the karst cave, with minimum displacement on the monitoring section of 30 m. When the tunnel depth is 300, 400 or 500 m, the Y-displacement of tunnel vault monitoring point #1 shows a clear change, with the

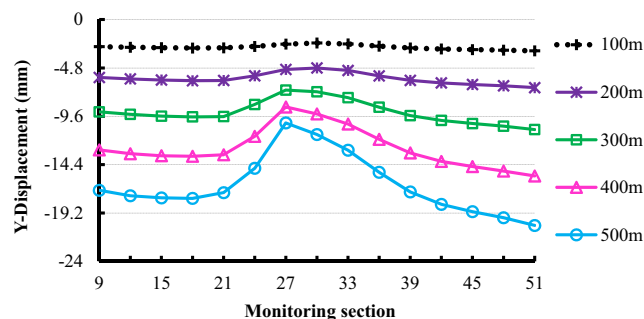


Fig. 5 The Y-displacement of tunnel vault monitoring point #1 at different tunnel depths

greatest change occurring in the vicinity of the karst cave. The lowest displacement occurring on the monitoring section of 27 m.

- 3) Overall, as the excavation length increases, the Y-displacement of tunnel vault monitoring point #1 first decreases and then increases, and its direction is downward. Moreover, the displacement changes greatly near by the karst cave, which is an obvious turning point. The reason for this change is: in the vicinity of the top karst cave, the surrounding rock in tunnels produces convergence towards the free face of the karst cave due to the impact of the karst cave, which reduces the Y-displacement of tunnel vault monitoring point #1; the closer the excavation is to the karst cave, the greater the displacement variation.

The X-displacement of tunnel haunch monitoring points #2 and #4

Horizontal displacements (X-displacement) of tunnel haunch monitoring points #2 and #4 are symmetrical, and only their directions are reversed. The displacement rules of the above two monitoring points are the same. Therefore, the X-displacement of monitoring point #2 is taken as an example. In the course of tunnel excavation, the horizontal displacement of tunnel haunch monitoring point #2 on each monitoring section is monitored and drawn in curves. The X-displacement diagram of tunnel haunch monitoring point #2 at different tunnel depths is then obtained, as shown in Fig. 6.

- a) With increasing tunnel depth, the X-displacement of monitoring point #2 increases gradually, as does the range.
- b) On the whole, the X-displacement of tunnel haunch monitoring point #2 gently changes, and its direction is toward the right. The displacement variation of monitoring point #2 shows an approximate tendency toward the horizontal line when the tunnel depth is smaller.

The Y-displacement of tunnel bottom monitoring point #3

In the course of tunnel excavation, the vertical displacement of

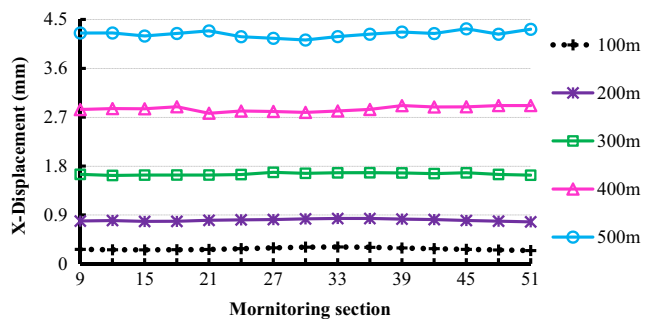


Fig. 6 The X-displacement of the tunnel haunch monitoring point #2 at different tunnel depths

the tunnel bottom monitoring point #3 on each monitoring section is monitored and drawn in curves. The Y-displacement diagram of tunnel bottom monitoring point #3 at different tunnel depths is then obtained, as shown in Fig. 7.

- a. With increasing tunnel depth, the Y-displacement of monitoring point #3 increases gradually, as does the extent of variation.
- b. Overall, as the excavation length increases, the Y-displacement of tunnel bottom monitoring point #3 first decreases and then increases, and its direction is upward. Specifically, in the vicinity of the top karst cave, the Y-displacement of tunnel bottom monitoring point #3 slightly decreases owing to the impact of the karst cave, reaching its minimum on the monitoring section of 33 m.

The second class of case studies—different surrounding rock grades

A karst cave is built on the top of the planned tunnel, and its center is located at the middle section of the model in the Z-direction. The range of the top karst cave in the Z-direction is from -24 m to -36 m. In order to investigate the stability of the surrounding rock in tunnels affected by the top concealed karst cave under different surrounding rock grades, the surrounding rock grade is set at grade I, grade II, grade III, grade IV and grade V, respectively. Median values for the other four influencing factors are chosen and remain unchanged during the modeling, i.e., tunnel depth (300 m), side length of the karst cave (12 m), distance between the tunnel and the karst cave (6 m) and depth-span ratio of the karst cave (1:1).

The Y-displacement of tunnel vault monitoring point #1

The Y-displacement diagram of tunnel vault monitoring point #1 under different surrounding rock grades is shown in Fig. 8.

- 1) With a reduction in the grade of the surrounding rock, the Y-displacement of monitoring point #1 increases gradually, as do the range and the extent of variation.

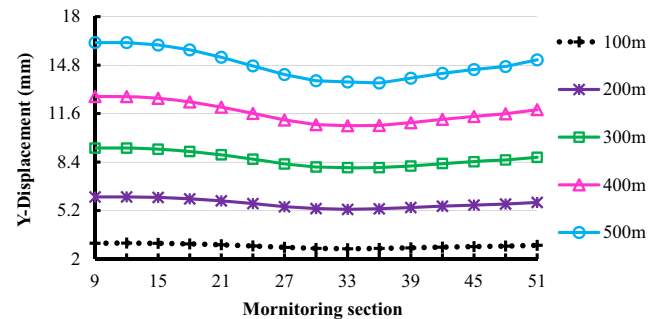


Fig. 7 The Y-displacement of tunnel bottom monitoring point #3 at different tunnel depths

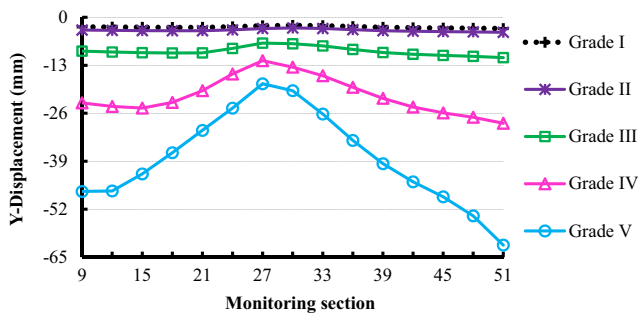


Fig. 8 The Y-displacement of tunnel vault monitoring point #1 under different surrounding rock grades

- When surrounding rock of the tunnel is grade I or grade II, the Y-displacement of tunnel vault monitoring point #1 changes gently. The displacement decreases slightly nearby the karst cave, reaching a minimum in the monitoring section of 30 m. As for the surrounding rock of grade III, when the range of monitoring section is from 9 to 18 m, the Y-displacement of tunnel vault monitoring point #1 changes gently and shows an increase tendency. When the range of monitoring section is from 18 to 27 m, the Y-displacement of monitoring point #1 gradually decreases and reaches its minimum on the monitoring section of 27 m. After crossing the position of the karst cave center, i.e., when the range of monitoring section is from 27 to 51 m, the Y-displacement of monitoring point #1 increases gradually, reaching its maximum value on the monitoring section of 51 m. As for the surrounding rock of grade IV, when the range of monitoring section is from 9 to 15 m, the Y-displacement of tunnel vault monitoring point #1 increases gradually. When the range of monitoring section is from 15 to 27 m, the Y-displacement of monitoring point #1 decreases gradually, reaching its minimum on the monitoring section of 27 m. After crossing the position of the karst cave center, i.e., when the range of monitoring section is from 27 to 51 m, the Y-displacement of monitoring point #1 increases gradually, reaching its maximum on the monitoring section of 51 m. Regarding the surrounding rock of grade V, when the range of monitoring section is from 9 to 27 m, the Y-displacement of monitoring point #1 decreases gradually, reaching its minimum on the monitoring section of 27 m. After crossing the position of the karst cave center, i.e., when the range of monitoring section is from 27 to 51 m, the Y-displacement of monitoring point #1 increases gradually, reaching its maximum on the monitoring section of 51 m.
- Overall, as the excavation length increases, the Y-displacement of tunnel vault monitoring point #1 first decreases and then increases, and its direction is downward. Moreover, the displacement changes greatly nearby the karst cave, which is an obvious turning point. The reasons are as follows: in the vicinity of the top karst cave, the surrounding rock in tunnels convergence towards the

free face of the karst cave due to the impact of the karst cave, which in turn reduces the Y-displacement of tunnel vault monitoring point #1.

The X-displacement of tunnel haunch monitoring point #2

The X-displacement diagram of tunnel haunch monitoring point #2 under different surrounding rock grades is shown in Fig. 9.

- With a reduction in the grade of the surrounding rock grade, the X-displacement of monitoring point #2 gradually increases, as does the increasing range.
- When the surrounding rock grade is grade I, grade II or grade III, the X-displacement of tunnel haunch monitoring point #2 is smaller and shows an approximate tendency toward a horizontal line. For the surrounding rock of grade IV or grade V, when the range of monitoring section is from 9 to 30 m, the X-displacement of monitoring point #2 decreases gradually, reaching its minimum on the monitoring section of 30 m. When the range of monitoring section is from 30 to 51 m, the X-displacement of monitoring point #2 increases gradually, reaching its maximum on the monitoring section of 51 m.
- Overall, when the surrounding rock grade is higher (grade I, grade II or grade III), the X-displacement of tunnel haunch monitoring point #2 is less affected by the top karst cave. To the contrary, when the surrounding rock grade is lower (grade IV or grade V), the top karst cave has a greater effect on the X-displacement of tunnel haunch monitoring point #2, thereby reducing X-displacement.

The Y-displacement of the tunnel bottom monitoring point #3

The Y-displacement diagram of tunnel bottom monitoring point #3 under different surrounding rock grades is shown in Fig. 10.

- With a reduction in the grade of the surrounding rock grade, the Y-displacement of monitoring point #3 increases gradually, as doe the range and the extent of variation.

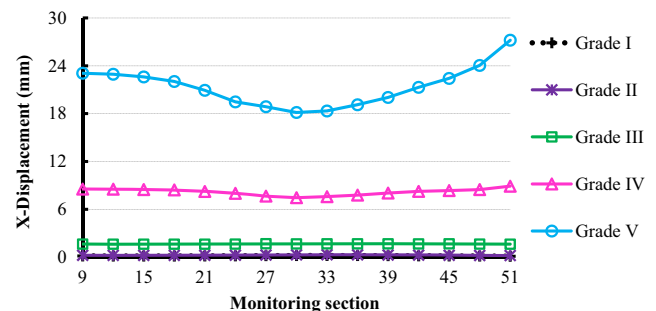


Fig. 9 The X-displacement of the tunnel haunch monitoring point #2 under different surrounding rock grades

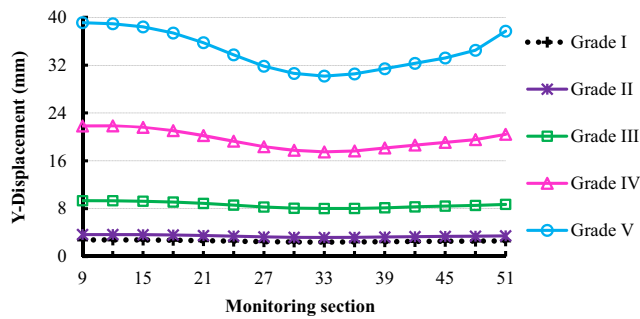


Fig. 10 The Y-displacement of the tunnel bottom monitoring points #3 under different surrounding rock grades

- Overall, owing to the impact of the top karst cave, as the excavation length increases, the Y-displacement of the tunnel bottom monitoring point #3 first decreases and then increases, reaching its minimum on the monitoring section of 33 m. The direction of the Y-displacement is upward. Specifically, the Y-displacement of monitoring point #3 decreases gradually when the range of the monitoring section is from 9 to 33 m, and the displacement increases gradually when the range of the monitoring section is from 33 to 51 m.

The third class of case studies—different sizes of the concealed karst cave

A karst cave is built on the top of the planned tunnel, and its center is located at the middle section of the model in the Z-direction. In order to investigate the stability of surrounding rock in tunnels affected by the sizes of the concealed karst cave, the side length of the karst cave is set to 4, 8, 12, 16 and 20 m, respectively. The median values of the other four influencing factors are chosen and these remain unchanged during the modeling, i.e., tunnel depth (300 m), surrounding rock grade (Grade III), the distance between the tunnel and the karst cave (6 m), depth–span ratio of the karst cave (1:1).

The Y-displacement of tunnel vault monitoring point #1

The Y-displacement diagram of tunnel vault monitoring point #1 under different sizes of the concealed karst cave is shown in Fig. 11.

- With increasing volume of the karst cave, the change range of the Y-displacement of monitoring point #1 increases gradually.
- When there is no concealed karst cave, with increasing excavation length the Y-displacement of tunnel vault monitoring point #1 changes gently and shows a tendency to increase. Specifically, the Y-displacement is a minimum (−8.935 mm) on the monitoring section of 9 m

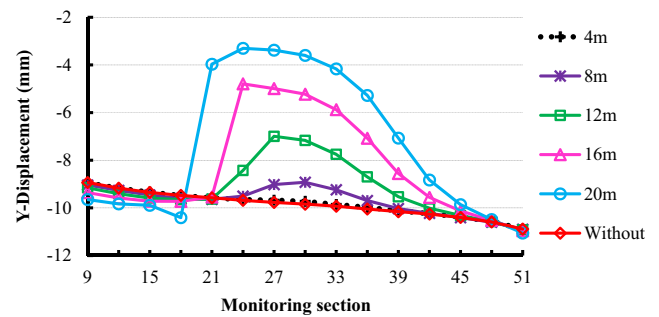


Fig. 11 The Y-displacement of tunnel vault monitoring point #1 under different sizes of the concealed karst cave

- and a maximum (−10.89 mm) on the monitoring section of 51 m. When the side length of the karst cave is 4 m, the Y-displacement variation of monitoring point #1 is basically the same as that without the karst cave, and it also has a tendency of increase. The difference of the Y-displacement is smaller between the two, and the corresponding change curves are in good agreement. As for the side length of 8 m, when the range of the monitoring section is from 9 to 21 m, the Y-displacement of tunnel vault monitoring point #1 increases gradually. When the range of the monitoring section is from 21 to 30 m, the Y-displacement of monitoring point #1 decreases gradually, reaching its minimum on the monitoring section of 30 m. When the range of monitoring section is from 30 to 51 m, the Y-displacement of monitoring point #1 increases, reaching its maximum on the monitoring section of 51 m. As for the side length of 12 m, when the range of the monitoring section is from 9 to 18 m, the Y-displacement of tunnel vault monitoring point #1 increases gradually. When the range of the monitoring section is from 18 to 27 m, the Y-displacement of monitoring point #1 decreases gradually, reaching its minimum on the monitoring section of 27 m. After crossing the position of the karst cave center, i.e., when the range of the monitoring section is from 27 to 51 m, the Y-displacement of monitoring point #1 increases gradually, reaching its maximum on the monitoring section of 51 m. As for the side length of 16 or 20 m, when the range of the monitoring section is from 9 to 18 m, the Y-displacement of tunnel vault monitoring point #1 increases gradually. When the range of the monitoring section is from 18 to 24 m, the Y-displacement of monitoring point #1 decreases gradually, reaching its minimum on the monitoring section of 24 m. When the range of the monitoring section is from 24 to 51 m, the Y-displacement of monitoring point #1 increases gradually, reaching its maximum on the monitoring section of 51 m.
- Overall, the Y-displacement of tunnel vault monitoring point #1 decreases to some extent in the vicinity of the top karst cave, which is an obvious turning point.

Moreover, as the volume of the karst cave increases, the Y-displacement of monitoring point #1 gets smaller and smaller. In addition, compared with the case study without the karst cave, when the volume of the karst cave is smaller ($a = 4$ m), the variation in Y-displacement of monitoring point #1 is basically the same as that without the karst cave. As the volume of the karst cave increases ($a = 8, 12, 16, 20$ m), the extent of the Y-displacement variation also increases gradually. The corresponding change rates are all significantly larger than that without the karst cave. In summary, the larger the volume of the karst cave, the more obvious the differences with the case study.

The X-displacement of tunnel haunch monitoring point #2

The X-displacement diagram of the tunnel haunch monitoring point #2 under different sizes of the concealed karst cave is shown in Fig. 12.

- 1) With increasing volume of the karst cave, the X-displacement of the monitoring point #2 increases gradually.
- 2) On the whole, as the excavation length increases, the X-displacement of tunnel haunch monitoring point #2 changes slightly, with slight fluctuations nearby the karst cave. Compared with the case study without the karst cave, when the side length of the karst cave is 4 or 8 m, the corresponding X-displacement is scarcely different from that without the karst cave. When the side length of the karst cave is 12, 16 or 20 m, its corresponding X-displacement is more than the X-displacement without the karst cave. In other words, when the volume of the karst cave is larger, the top karst cave has a larger effect on the X-displacement of tunnel haunch monitoring point #2, resulting in increased X-displacement.

The Y-displacement of tunnel bottom monitoring point #3

The Y-displacement diagram of tunnel bottom monitoring point #3 under different sizes of the concealed karst cave is shown in Fig. 13.

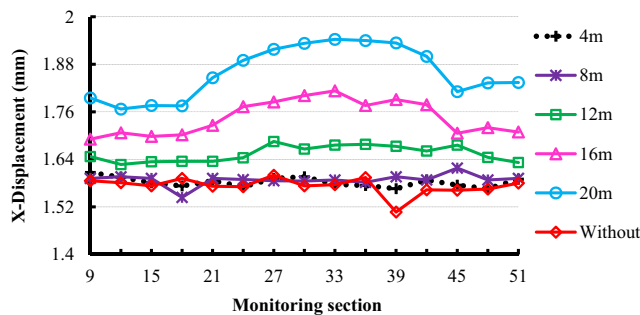


Fig. 12 The X-displacement of tunnel haunch monitoring points #2 under different sizes of the concealed karst cave

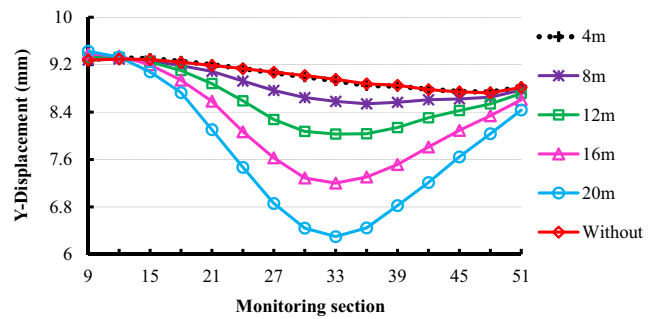


Fig. 13 The Y-displacement of the tunnel bottom monitoring points #3 under different sizes of the concealed karst cave

- 1) With increasing volume of the karst cave, the variation in the range of the Y-displacement of monitoring point #3 also increases gradually.
- 2) When there is no concealed karst cave, with increasing excavation length, the Y-displacement of tunnel bottom monitoring point #3 changes gently and shows a decreasing tendency. When the side length of the karst cave is 4 m, the Y-displacement variation of monitoring point #3 is basically the same as that without the karst cave. The difference of the Y-displacement is small between these two conditions, and the corresponding change curves are in good agreement. As for the side length of 8 m, when the range of the monitoring section is from 9 to 36 m, the Y-displacement of tunnel bottom monitoring point #3 decreases gradually, reaching its minimum on the monitoring section of 36 m. When the range of monitoring section is from 36 to 51 m, the Y-displacement of monitoring point #3 gradually increases. Regarding the side length of 12, 16 or 20 m, when the range of the monitoring section is from 9 to 33 m, the Y-displacement of tunnel bottom monitoring point #3 decreases gradually, reaching its minimum on the monitoring section of 33 m. When the range of the monitoring section is from 33 to 51 m, the Y-displacement of monitoring point #3 gradually increases.
- c) Overall, the Y-displacement of tunnel bottom monitoring point #3 decreases to some extent under the influence of the top karst cave, which is an obvious turning point. Moreover, as the volume of the karst cave increases, the Y-displacement of monitoring point #3 gets smaller and smaller. In addition, compared with the case study without the karst cave, when the volume of the karst cave is smaller ($a = 4$ m), the variation in Y-displacement of monitoring point #3 is basically the same as that without the karst cave. As the volume of the karst cave increases ($a = 8, 12, 16, 20$ m), the extent of the variation in Y-displacement also increases gradually. The corresponding change rates are all significantly larger than that without the karst cave. In summary, the larger the volume of the karst cave, the more obvious the differences with the case study.

The fourth class case studies—different distances between the tunnel and the concealed karst cave

A karst cave is built on the top of the planned tunnel, and its center is located at the middle section of the model in the Z-direction. The range of the top karst cave in the Z-direction is from -24 m to -36 m. In order to investigate the stability of surrounding rock in tunnels affected by the distances between the tunnel and the concealed karst cave, the distance is set to 2, 4, 6, 8 and 10 m, respectively. The median values of the other four influencing factors are chosen, and these remain unchanged during the modeling, i.e., tunnel depth (300 m), surrounding rock grade (Grade III), the side length of the karst cave (12 m) and depth–span ratio of the karst cave (1:1).

The Y-displacement of tunnel vault monitoring point #1

The Y-displacement diagram of the tunnel vault monitoring point #1 under different distances is shown in Fig. 14.

- 1) With increasing distance, the variation in the range of the Y-displacement of monitoring point #1 decreases gradually.
- 2) Overall, the Y-displacement of tunnel vault monitoring point #1 decreases to some extent in the vicinity of the top karst cave, which is an obvious turning point. Moreover, as the distance decreases, the Y-displacement of monitoring point #1 gets smaller and smaller. In addition, compared with the case study without the karst cave, as the distance decreases, the extent of the Y-displacement variation gradually increases. The corresponding change rates are all significantly larger than that without the karst cave. In summary, the smaller the distance between the tunnel and the karst cave, the more obvious the differences.

The X-displacement of tunnel haunch monitoring point #2

The X-displacement diagram of tunnel haunch monitoring point #2 under different distances is shown in Fig. 15.

- 1) With increasing distance, the X-displacement of monitoring point #2 decreases gradually.

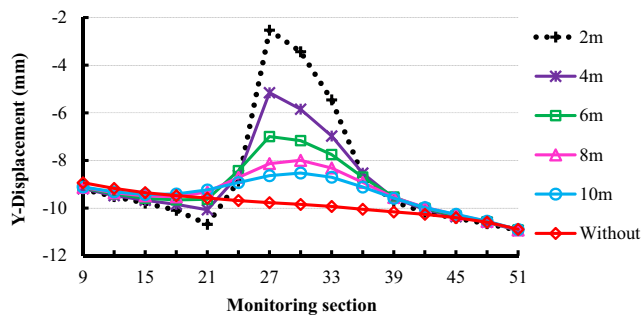


Fig. 14 The Y-displacement of tunnel vault monitoring point #1 under different distances

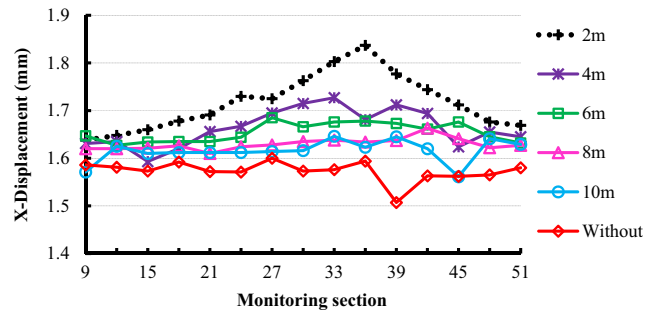


Fig. 15 The X-displacement of tunnel haunch monitoring point #2 under different distances

- 2) On the whole, as the excavation length increases, the X-displacement of tunnel haunch monitoring point #2 changes slightly, and the variation of total displacement is also slight. Compared with the case study without the karst cave, the X-displacement of monitoring point #2 under the five distances is more than the that without the karst cave. Moreover, in the vicinity of the karst cave, where the distance between the tunnel and the karst cave is smaller (2 and 4 m), the X-displacement of tunnel haunch monitoring point #2 affected by the top karst cave is larger, resulting in increased X-displacement.

The Y-displacement of tunnel bottom monitoring point #3

The Y-displacement diagram of tunnel bottom monitoring point #3 under different distances is shown in Fig. 16.

- 1) With increasing distance, the range in variation of the Y-displacement of monitoring point #3 decreases gradually.
- 2) On the whole, the Y-displacement of tunnel vault monitoring point #3 decreases to some extent in the vicinity of the top karst cave, which is an obvious turning point. Moreover, as the distance decreases, the Y-displacement of monitoring point #3 gets smaller and smaller. In addition, compared with the case study without the karst cave, as the distance decreases, the extent of the Y-displacement variation gradually increases. The corresponding change

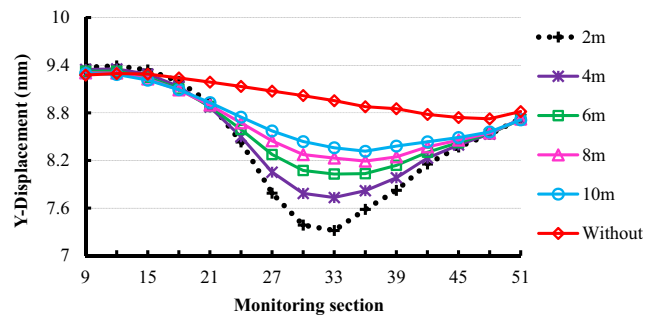


Fig. 16 The Y-displacement of the tunnel bottom monitoring points #3 under different distances

rates are all significantly larger than that without the karst cave. In summary, the smaller the distance between the tunnel and the karst cave, the more obvious the differences.

The fifth class case studies—different depth-span ratio of the concealed karst carve

A karst cave is built on the top of the planned tunnel, and its center is located at the middle section of the model in the Z-direction. The range of the top karst cave in the Z-direction is from -24 m to -36 m. In order to investigate the stability of surrounding rock in tunnels affected by the depth-span ratio of the concealed karst carve, based on the constant-volume principle, the depth-span ratio is set to 6:24, 8:18, 12:12, 18:8 and 24:6, respectively. The median values of the other four influencing factors are chosen, and these remain unchanged, i.e., tunnel depth (300 m), surrounding rock grade (Grade III), the side length of the karst cave in the Z-direction (12 m) and the distance between the tunnel and the karst cave (6 m).

The Y-displacement of tunnel vault monitoring point #1

The Y-displacement diagram of tunnel vault monitoring point #1 under different depth-span ratios is shown in Fig. 17.

- 1) With increasing depth-span ratio, the range in variation of the Y-displacement of monitoring point #1 decreases gradually.
- 2) Overall, the Y-displacement of tunnel vault monitoring point #1 decreases to some extent in the vicinity of the top karst cave, which is an obvious turning point. Moreover, as the depth-span ratio decreases, the Y-displacement of monitoring point #1 gets smaller and smaller. In addition, compared with the case study without the karst cave, the total change rates of the Y-displacement under the five depth-span ratios are all larger. In summary, the smaller the depth-span ratio, the larger the change rate and more distinct the differences.

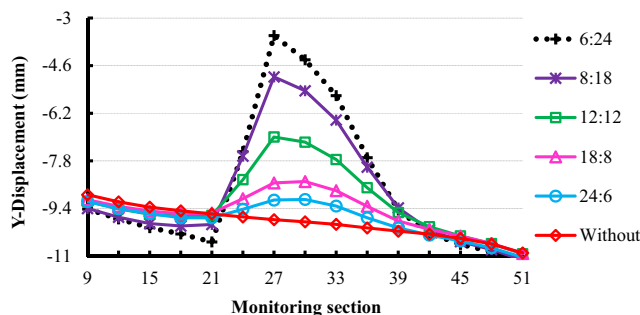


Fig. 17 The Y-displacement of the tunnel vault monitoring point #1 under different depth-span ratios

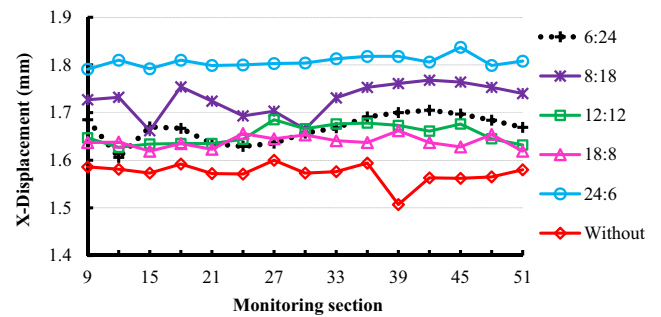


Fig. 18 The X-displacement of tunnel haunch monitoring point #2 under different depth-span ratios

The X-displacement of tunnel haunch monitoring point #2

The X-displacement diagram of tunnel haunch monitoring points #2 under different depth-span ratios is shown in Fig. 18.

- 1) The X-displacement of monitoring point #2 is maximum when the depth-span ratio is 24:6.
- 2) Overall, with increasing excavation length, the X-displacement of tunnel haunch monitoring point #2 changes slightly, and the variation of total displacement is also slight. Compared with the case study without the karst cave, the X-displacement of monitoring point #2 under the five depth-spans ratio is greater. However, as the depth-span ratio changes, the X-displacement variation of monitoring point #2 shows no obvious regularity.

The Y-displacement of tunnel bottom monitoring point #3

The Y-displacement diagram of tunnel bottom monitoring point #3 under different depth-span ratios is shown in Fig. 19.

- 1) With increasing depth-span ratio, the range of variation of the Y-displacement of monitoring point #3 decreases gradually.
- 2) Overall, the Y-displacement of tunnel vault monitoring point #3 decreases to some extent in the vicinity of the top karst cave, which is the obvious turning

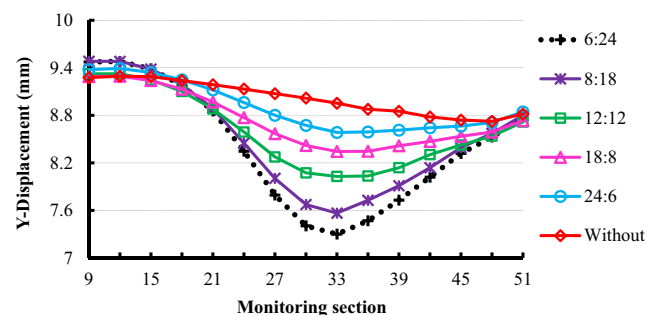


Fig. 19 The Y-displacement of tunnel bottom monitoring point #3 under different depth-span ratio

point. Moreover, as the depth–span ratio decreases, the Y-displacement of the monitoring point #3 gets smaller and smaller. In addition, compared with the case study without the karst cave, the total change rates of the Y-displacement under the five depth–span ratio. In summary, the smaller the depth–span ratio, the larger the change rate and more obvious the differences.

Conclusions

A possible prediction method of the top concealed karst cave based on displacement monitoring during tunnel construction is investigated and proposed. We investigated displacement on monitoring surfaces after the tunnel is excavated once. The displacement laws of tunnel arch ring monitoring points are analyzed and discussed and then compared to a case study without karst caves. Based on the results of this analysis and discussion, we propose a possible engineering application method for predicting the top concealed karst cave.

In order to verify the proposed method, stepwise excavation was studied based on numerical simulation. Displacement laws of the tunnel arch ring monitoring points under different monitoring distances (3, 6, 9 and 12 m) were analyzed. Moreover, the tunnel depth, the surrounding rock grade, the size of the concealed karst cave, the distance between the tunnel and the concealed karst cave and the depth–span ratio of the concealed karst cave were selected as research targets based on the stepwise excavation. For each influencing factor, five additional case studies were simulated and investigated. The impacts of these factors on the stability of surrounding rock in tunnels were studied by considering the displacement field. The surrounding rock deformation affected by the top karst cave during tunnel excavation was compared with the case study without the karst cave. The simulation results were consistent with those predicted by the proposed method.

The following conclusions are drawn:

- (1) With increasing monitoring distance, the displacements of the tunnel arch ring monitoring points also increase gradually, but the increasing range decreases gradually.
- (2) With increasing tunnel depth, Y-displacement of both tunnel vault monitoring point #1 and tunnel bottom monitoring point #3 increase gradually, as does the extent of variation. The X-displacement of tunnel haunch monitoring point #2 increases with the tunnel depth, and the increasing range also increases gradually.
- (3) With reduction of the surrounding rock grade, Y-displacement of both tunnel vault monitoring point

#1 and tunnel bottom monitoring point #3 increase gradually, as do the increasing range and extent of variation. The X-displacement of tunnel haunch monitoring point #2 increases as the surrounding rock grade reduces, and the increasing range also increases gradually.

- (4) With increasing volume of the concealed karst cave, the changes of Y-displacement of both tunnel vault monitoring point #1 and tunnel bottom monitoring point #3 increase gradually. Nearby the karst cave, the larger the volume of the karst cave, the smaller the Y-displacement.
- (5) With increasing distance between the tunnel and the concealed karst cave, the changes of Y-displacement of both tunnel vault monitoring point #1 and tunnel bottom monitoring point #3 decrease gradually. Nearby the karst cave, the smaller the distance between the tunnel and the karst cave, the smaller the Y-displacement.
- (6) With increasing depth–span ratio of the concealed karst cave, the changes of Y-displacement of tunnel vault monitoring point #1 and tunnel bottom monitoring point #3 both decrease gradually. Nearby the karst cave, the smaller the depth–span ratio of the karst cave, the smaller the Y-displacement.
- (7) During the tunnel excavation, the top concealed karst cave causes a decrease in the Y-displacement of both tunnel vault monitoring point #1 and tunnel bottom monitoring point #3. The closer to the karst cave, the greater the Y-displacement variation.
- (8) Among these the five influencing factors studied, in terms of impact on the deformation of surrounding rock in tunnels, the displacement of the tunnel vault was most affected by the top concealed karst cave, followed by the tunnel bottom; the tunnel haunch was the least affected.

Acknowledgments We would like to acknowledge the financial support from the National Basic Research Program of China (973 Program, No.: 2013CB036000), the National Natural Science Foundation of China (Grant Nos.: 51509147, 51379114) and the promotive research fund for excellent young and middle-aged scientists of Shandong Province (Grant No.: 2014BSE27132).

References

- Cai MF, He MC, Liu DY (2002) Rock mechanics and engineering. Science Press, Beijing
- Chen CZ, He FL (2004) Tunnel engineering geology and acoustic detection technology. Southwest Jiaotong University Press, Chengdu
- Chen WZ, Zhu WS, Shao JF (2004) Damage coupled time-dependent model of a jointed rock mass and application to large underground cavern excavation. *Int J Rock Mech Min* 41(4):669–677

- Cooper AH (1998) Subsidence hazards caused by the dissolution of Permian gypsum in England: geology, investigation and remediation. In: Maund JG, Eddleston M (eds.) *Geohazards in engineering geology. Special publications in engineering geology*, vol 15. Geological Society of London, London, pp 265–275.
- Day MJ (2004) Karstic problems in the construction of Milwaukee's deep tunnels. *Environ Geol* 45(6):859–863
- Fu KL, Feng T (2012) Characteristics of karst cave in Beiya tunnel of Guangxi-Guizhou railway and the treatment measures. *Subgrade Eng* 2:155–158+162
- Fu J, Yang J, Klapperich H, Wang S (2015) Analytical prediction of ground movements due to a Nonuniform deforming tunnel. *Int J Geomech* 16(4):04015089. doi:10.1061/(ASCE)GM.1943-5622.0000580
- Gutierrez F, Parise M, De Waele J, Jourde H (2014) A review on natural and human-induced geohazards and impacts in karst. *Earth-Sci Rev* 138:61–88
- Hu QF, Huang HW (2007) Numerical analysis and risk assessment on face stability of large-diameter tunnels. *Computational Science–ICCS 2007*. Springer, Berlin Heidelberg, pp 1180–1187
- Knez M, Slabe T (2002) Karstology and the opening of caves during motorway construction in the karst region of Slovenia. *Int J Speleol* 31(1):9
- Lai YB, (2012) Study on safe distance between concealed karst cave and tunnel and its intelligent prediction model. PhD dissertation, Beijing Jiaotong University, Beijing
- Li SC, Wu J, Xu ZH, Li LP, Huang X, Xue YG, Wang ZC (2016) Numerical analysis of water flow characteristics after intruding from the tunnel floor in process of karst tunnel excavation. *Geomech Eng* 10(4):471–526
- Liu DM, Yuan RM, Shang YJ, Bao WX, Wang KY, Zhang ZJ, Li K, He WT (2017) Deformation and failure of a tunnel in the restraining bend of a strike-slip fault zone: an example from Hengshan Mountain, Shanxi Province, China. *B Eng Geol Environ* 76(1):263–274
- Liu ZK, Liang JC, Zhu SZ, Zhang GL (2003) Stability analysis of rock foundation with cave in karst area. *Chinese J Geotech Eng* 25(5):629–633
- Liu J, Li ZK, Zhang ZY (2004) Stability analysis of block in the surrounding rock mass of a large underground excavation. *Tunn Undergr Sp Tech* 19(1):35–44
- Liu QS, Bai SY, Xiao CX, Gao W (2007) Study on surrounding rock stability of Longtan tunnel based on in-situ monitoring measurements. *Chinese J Rock Mech Eng* 26(10):1982–1990
- Mo YC (2009) Stability research on high water pressure filled karst caves tunnel. PhD dissertation, Southwest Jiaotong University, Xi'an
- Mo YC, Zhou XJ (2008) Dynamic monitoring and simulation analysis of surrounding rock deformation of tunnel in karst region. *Chinese J Rock Mech Eng* 27[Suppl. 2]:3816–3820
- Pan QJ, Dias D (2015) Face stability analysis for a shield-driven tunnel in anisotropic and nonhomogeneous soils by the kinematical approach. *Int J Geomech* 16(3):04015076. doi:10.1061/(ASCE)GM.1943-5622.0000569
- Parise M, Lollino P (2011) A preliminary analysis of failure mechanisms in karst and man-made underground caves in southern Italy. *Geomorphology* 134(1):132–143
- Runqiu H, Huabo X (2010) Deformation mechanism of a shallow double-arch tunnel in a sloping rock mass. *B Eng Geol Environ* 69(1):89–97
- Shrestha PK, Panthi KK (2015) Assessment of the effect of stress anisotropy on tunnel deformation in the Kaligandaki project in the Nepal Himalaya. *B Eng Geol Environ* 74(3):815–826
- Song ZP (2006) Research on the influence of concealed karst caves upon the stability of tunnels and its support structure. *Chinese J Rock Mech Eng* 25(6):1296
- Song ZP, Dang HB, Li N (2008) Numerical experimentation of influence of karst cave on displacement characteristics of rock mass. *J Yangtze River Sci Res Inst* 25(5):79–83
- Sterpi D, Cividini A (2004) A physical and numerical investigation on the stability of shallow tunnels in strain softening media. *Rock Mech Rock Eng* 37(4):277–298
- Tan DM, Qi TY, Mo YC (2009) Numerical analysis and research on surrounding rock stability of lateral cave tunnel. *Chinese J. Rock Mech. Eng.* 28[Suppl 2]:3497–3503
- Taromi M, Eftekhari A, Hamidi JK and Aalianvari A (2016) A discrepancy between observed and predicted NATM tunnel behaviors and updating: a case study of the Sabzkuh tunnel. *B Eng Geol Environ* 1–17. doi:10.1007/s10064-016-0862-x
- Wang TL, Fan QY (2000) Optimization of soft rock engineering with particular reference to coal mining. *Int J Rock Mech Min* 37(3):535–542
- White WB (2002) Karst hydrology: recent developments and open questions. *Eng Geol* 65(2):85–105
- Xu ZM, Huang RQ, Zhang ZY (2001) The mechanical parameters of surrounding rocks considered in TBM cutter design. *Chinese J Rock Mech Eng* 20(2):230–234
- Yang JS, Liu BC, Wang MC (2004) Modeling of tunneling-induced ground surface movements using stochastic medium theory. *Tunn Undergr Sp Tech* 19(2):113–123
- Zhao MJ, Ao JH, Liu XH, Wang B (2004) Model testing research on influence of karst cave size on stability of surrounding rock masses during tunnel construction. *Chinese J Rock Mech Eng* 23(2):213–217
- Zhao YL, Peng QY, Wan W, Wang WJ, Chen B (2014) Fluid–solid coupling analysis of rock pillar stability for concealed karst cave ahead of a roadway based on catastrophic theory. *Int J Min Tech* 24(6):737–745
- Zou CJ (1994) Water resources and hydropower karst engineering geology. China Waterpower Press, Beijing